Check for updates

Enhancing antioxidant and bioactive metabolite production in *Carthamus tinctorius* cell suspension culture through nano-elicitor mediated elicitation

Kamran Ashraf,[a] Qamar uz Zaman, [b] Yu Liu,[a] Senyi Gong,[a] Aimon Saleem,[b] Muhammad Arshad, [c] Maria Martuscelli,[d] Nazih Y. Rebouh,[e] Meijin Guo [*a] and Ali Mohsin*[a]

In this study, Se-doped $CeO_2@Fe_3O_4$ nanoparticles (NPs) were synthesized and applied to a *Carthamus tinctorius* (safflower) cell suspension culture using liquid medium (B5). The application of these NPs at various levels (0, 5, 10, 15 and 20 mg L^{-1}) was studied for its effects on cell growth, physio-biochemical traits and antioxidative activities. The addition of NPs to the culture media significantly improved the cell biomass, antioxidant potential and phenolic contents. The addition of NPs at the rate of 15 mg L^{-1} (T_3 treatment group) significantly improved the dry biomass of cells (128.72%), total chlorophyll contents (76.02%), and reduced levels of hydrogen peroxide (5.15%) and reactive oxygen (26.51%) compared to the control group (0 mg L^{-1}). Furthermore, this study identified 29 differentially expressed genes (DEGs) in the jasmonate signalling pathway. Notably, only the two DEGs from the *MYC2* family showed mixed expression at different time points (6 h, 24 h, 48 h, and 72 h) following treatment with Se-doped $CeO_2@Fe_3O_4$ NPs. In conclusion, these findings demonstrate that this approach is effective, adaptable, biocompatible, and cost-efficient, offering a promising strategy for enhancing the production of antioxidant and bioactive metabolites in industrial-scale safflower cultivation.

1. Introduction

Carthamus tinctorius (*C. tinctorius*) is a perennial herb belonging to the *Asteraceae* (Compositae) family. It is characterized by its abundant secondary metabolites and phytochemicals, including carthamin (red pigment), safflower yellow pigments (hydroxysafflor yellow A, safflomin C), and polyunsaturated fatty acids (linoleic acid).[1] As an important industrial crop, it provides high-quality vegetable oil extracted from its seeds, which is used for cooking purposes.[2] The flowers serve as a source of natural dyes for the food and textile industries. Traditionally recognized for supporting cardiovascular health, *C. tinctorius* is now also valued for its potential health benefits attributed to compounds such as flavonoids and polyphenols.[3] Antioxidant enzymes, which are naturally present in plant cells, help to prevent damage caused by reactive oxygen species (ROS) by neutralizing free radicals.[4] Recently, plant cell culture methodology has been highlighted as a sustainable and effective approach for enhancing the antioxidative efficacy of plant-derived compounds. This process is also useful for acquiring antioxidants that are difficult to extract from plant sources.[5] Therefore, novel approaches such as nanoparticle (NP)-mediated elicitation and advanced genetic engineering methods are being used to improve the antioxidant production potential in safflower suspension culture.[6]

Elicitors are crucial for improving antioxidant production as they induce the natural defense mechanisms of the plant cells, leading to increased synthesis of protective compounds. These elicitors are classified as either biotic (microbial enzymes, or fungal or microbial elicitors) or abiotic (chemicals or NPs).[7] A wide variety of abiotic elicitors has been developed as effective tools to boost secondary metabolite production, with NPs demonstrating distinctive physical and chemical attributes, such as high surface area and controlled reactivity.[8] The NP mediated elicitation is characterized by the interaction between NPs and plant cells, which triggers the localized ROS generation. This interaction subsequently activates specific signal transduction pathways that regulate the expression of antioxidants.[9] Consequently, these pathways specifically induce enzymes involved in antioxidant biosynthesis, leading to an increased production of antioxidants.[10]

[a]*State Key Laboratory of Bioreactor Engineering, East China University of Science and Technology, Shanghai 200237, PR China. E-mail: alimohsin@ecust.edu.cn; guo_mj@ecust.edu.cn; Tel: +86 13162094883; +86 21 64253011; +86 21 64253702*

[b]*Department of Environmental Sciences, The University of Lahore, Lahore 54590, Pakistan*

[c]*Institute of Environmental Sciences and Engineering, School of Civil and Environmental Engineering, National University of Sciences and Technology (NUST), Sector H-12, Islamabad 44000, Pakistan*

[d]*Department of Bioscience and Food, Agricultural and Environmental Technology, University of the Studies of Teramo, Via Balzarini 1, 64100 Teramo (TE), Italy*

[e]*Institute of Environmental Engineering, RUDN University, 6 Miklukho-Maklaya St., Moscow 117198, Russia. E-mail: rebukh-nya@rudn.ru*

Inorganic elements such as iron, cerium, and selenium are trace elements that act as cofactors for antioxidant enzymes, including thioredoxin reductases and glutathione peroxidases.[11] Furthermore, NPs of these elements have demonstrated a significant impact on various biological functions, such as metabolic regulation and antioxidant synthesis, revealing their potential application as elicitors.[12] CeO_2 NPs scavenge reactive oxygen species (ROS) through the reversible redox cycling between Ce^{3+} and Ce^{4+} states. This mitigates oxidative damage and helps maintain cellular redox homeostasis.[13] This nanoparticle system is supported by Fe_3O_4, which enhances the Fe bioavailability to plant cells. This increased bioavailability boosts enzyme activities, leading to enhanced synthesis of antioxidants, ROS signaling, and cell metabolism. It was noticed that optimal level of FeO-NPs ($10–15$ mg L^{-1}) significantly enhanced callus growth attributes and metabolites production on solid Murashige and Skoog medium.[14] Similarly, selenium (Se) is integrated into seleno-proteins, which increases the overall antioxidative potential of the plant.[15] Conventional methods to regulate this antioxidative potential are often considered challenging in terms of their efficacy and feasibility.[16] In our previous reported works, we successfully synthesized unique Se-doped $CeO_2@Fe_3O_4$ and jasmonic acid (JA) loaded Fe_3O_4 NPs, and evaluated their efficacy at various levels in improving the secondary metabolites in cell culture of safflower.[4,17] Based on these observations, it was proposed that Se-doped $CeO_2@Fe_3O_4$ NPs can regulate enzymatic antioxidants and enhance the expression of secondary metabolites and genes associated with the jasmonate signaling pathway.

Research on enhancing secondary metabolites using doped NPs in safflower cell culture is still in its early stages, presenting significant opportunities to explore innovative techniques for improving antioxidative potential and increasing secondary metabolite production in safflower cell culture. To date, no prior research article is available in the literature on the effects of Se-doped $CeO_2@Fe_3O_4$ NPs on cell biomass formation and modulation of antioxidant potential in safflower suspension cultures. The objectives of the present investigation were: (a) to synthesize and analyze Se-doped $CeO_2@Fe_3O_4$ NPs to elucidate their physical and compositional traits; (b) to evaluate the variations in physio-biochemical attributes, enzymatic antioxidants, and ROS concentrations in safflower cells treated with various levels of these NPs; (c) to explore the elicitor induced/triggered transcriptional expression of key genes in safflower cells. The outcomes of this research highlight an innovative approach for producing Se-doped $CeO_2@Fe_3O_4$ NPs with enhanced stability and bioactivity. These NPs function as both elicitors and enhancers, establishing optimal conditions for improving biomass and enzymatic antioxidant profile. This study elucidates the underlying mechanisms, providing practical insights for enhancing antioxidative compounds to produce high-value bioactive metabolites.

2. Materials and methods

2.1. Synthesis and analysis of nanoparticles

The NPs were synthesized according to the protocols established in our previous study.[17] In detail, the Se-doped $CeO_2@Fe_3O_4$ NPs were prepared in three steps: (i) hydrothermal synthesis of Fe_3O_4 nanospheres, (ii) hydrothermal coating of CeO_2 followed by calcination and finally (iii) the terminal incorporation of Se by reducing sodium selenite using sodium borohydride with ethanol as a solvent. The surface morphology and crystal structure of synthesized NPs were determined by X-ray diffraction (XRD) analysis using an X'TRA showroom, (ARL Company, Switzerland). The internal structure was examined using transmission electron microscopy (TEM) images obtained with a JEM-2100CX microscope (JEOL Ltd., Japan). Particle morphology and elemental composition were analyzed *via* energy dispersive X-ray spectroscopy (EDX) using a Hitachi S-4800 FEG. The chemical states and surface chemistry were studied by X-ray photoelectron spectroscopy with a PHI 5000 Versa Probe instrument (ULVAC-PHI Ltd., Japan). Binding energies were calibrated using the C 1s photoelectron peak and analyzed with XPS Peak 4.1 software. The isoelectric point (IEP) was determined by plotting the zeta potential, which was measured using the Litesizer 500 photon correlation spectroscopy (Anton Paar GmbH, Austria). All the characterization measurements were performed in triplicate to ensure the reliability of the results.

2.2. Elicitation of *C. tinctorius* cells

Plant materials of *C. tinctorius* (safflower) were obtained from the country cultivation base in Yining, Xinjiang province, China. Explants were surface sterilized prior to callus induction using the following process: young branches were rinsed with distilled water to remove the dust, then dipped in sodium hypochlorite solution (4% v/v) for 15 minutes, followed by final rinse with sterilized water. The sterilized branch was dissected, and sections of sepals, leaves, stems and immature inflorescences were inoculated onto the callus induction medium. A suspension cell culture system was established using callus derived from inflorescence as described in our previous study[18] (Fig. 1). The *C. tinctorius* suspension cells were maintained in a liquid medium (B5) on a rotary shaker at 115 rpm for 6 days at 28 °C with 10% (m/v) inoculum. Se-doped $CeO_2@$ Fe_3O_4 NPs were added to the culture at varying doses ($T_0 = 0$ mg L^{-1}; $T_1 = 5$ mg L^{-1}; $T_2 = 10$ mg L^{-1}; $T_3 = 15$ mg L^{-1} and $T_4 = 20$ mg L^{-1}) and co-cultured for 3 days. To investigate levels of intracellular metabolites, cells were harvested every 24 h. The B5 medium consisted of B5 basal salt (3.21 g L^{-1}), α-naphthalene acetic acid (4×10^{-4} g L^{-1}), sucrose (30 g L^{-1}) and 6-benzylaminopurine (2×10^{-4} g L^{-1}). All the chemicals were purchased from Qingdao Hope Bio-Technology Co., Ltd, China.

2.3. Callus biomass, antioxidant metabolites, enzyme activities and transcriptome sequencing

To compare the growth dynamics of cell suspension cultures, fresh biomass was measured during seven days old cultures with the help of weighing balance. Cells were then harvested, dried at 50 °C, and weighed to determine the dry biomass.

For the evaluation of enzymatic antioxidants parameters, suspension cultures were assessed by using enzyme activity test kits from Solar Bio-Science & Technology (Beijing, China) Co.,
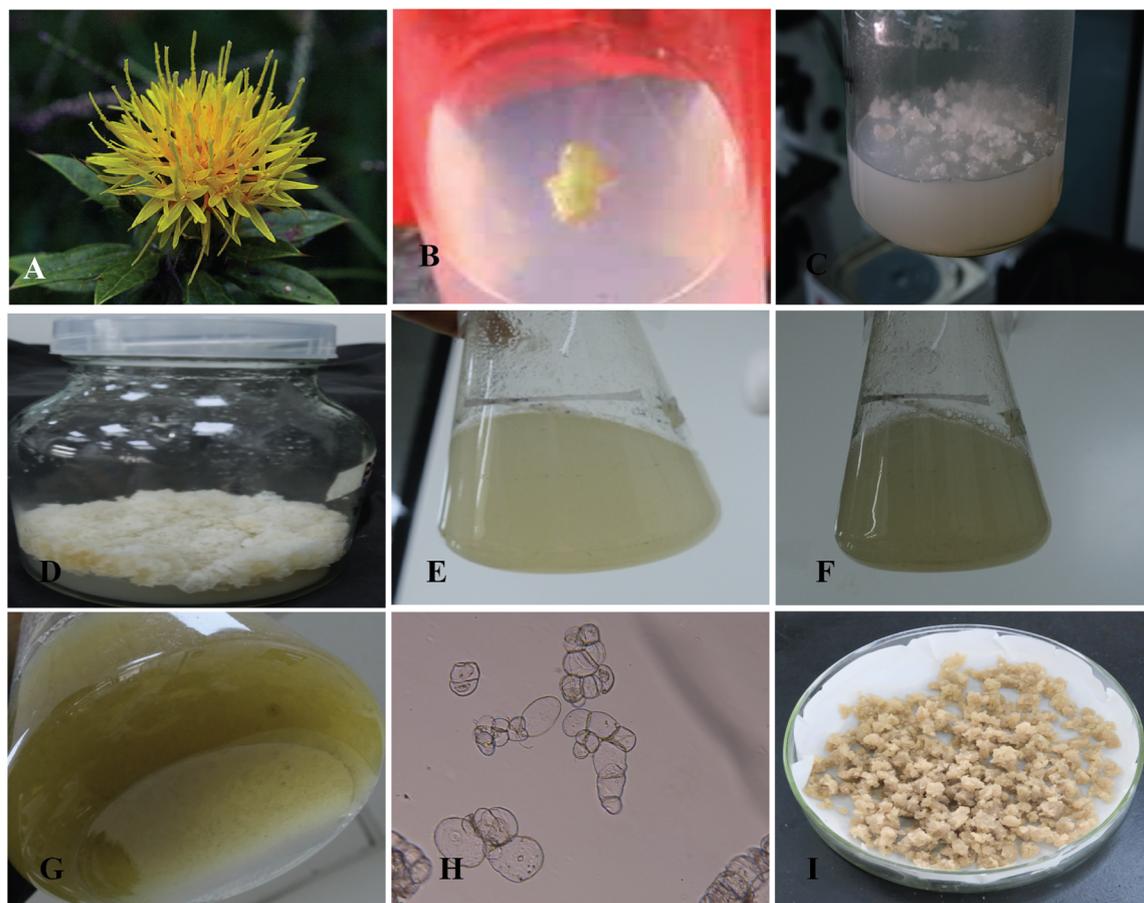
Fig. 1 Callus induction, suspension culture development and elicitation of *C. tinctorius* cells: (A) young branch of *C. tinctorius*; (B) calluses generated from the inflorescence; (C) embryo genic calluses initiated from the inflorescence; (D) embryogenic calluses cultured for 14 days; (E) *C. tinctorius* suspension cells of first generation; (F) *C. tinctorius* suspension cells after 5-time sub-culture; (G) *C. tinctorius* suspension cells after 3 days elicitation of nanoparticles; (H) morphology of *C. tinctorius* suspension cells under scanning electron microscope; (I) *C. tinctorius* suspension cells after vacuum filtration.

Ltd. These kits measured the activities of peroxidase (POD), superoxide dismutase (SOD), catalase (CAT), glutathione reductase (GR), and ascorbate peroxidase (APX). The experiments were conducted in accordance with manufacturer's guidelines. One unit of enzyme activity was defined as the change in absorbance at a specified wavelength per gram of tissue per minute per millimeter of the reaction system.[19] Furthermore, the soluble protein levels in the cultured cells were quantified utilizing the sulfuric acid anthrone colorimetric procedure and the Coomassie Brilliant Blue G250 protocol, as described by Peng *et al.*[19]

For pigment extraction about 0.4 g of cells were homogenized in 10 mL 80% acetone. The resulting solution was then filtered and centrifuged at 25 °C for 5 minutes at 5000×*g*. The absorbance of filtrate was measured using the spectrophotometric with chlorophyll *a* and *b* and carotenoids at 644.8 and 661.8 and 470 nm, respectively. The total chlorophyll contents were measured by adding chlorophyll *a* and *b* concentrations. The antioxidant profile of safflower extract was evaluated using ABTS and DPPH radical-scavenging assays, alongside a ferric ion reducing antioxidant power (FARP) study. This assessment

of antioxidant activity was conducted following previously described methodologies.[20,21]

For the measurement of reactive oxygen species related traits, the O_2^- contents were determined according to the method of Bu *et al.*[22] Briefly, approximately 0.1 g of cellular sample was homogenized in 2 mL of 50 mM phosphate buffer (pH 7.8) and centrifuged at 10 000*g* for 20 min. A 0.5 mL aliquot of supernatant was then incubated in a mixture containing 0.5 mL of 50 mM phosphate buffer (pH 7.8) and 1.5 mL of 1 mM hydroxylamine hydrochloride at 25 °C for 1 h. Subsequently, 2 mL of 2 mL of 17 mM *p*-aminobenzene sulfonic acid and 2 mL of 7 mM α-naphthylamine were added to the reaction mixture, which was incubated at 25 °C for 20 minutes, and absorbance was measured at 530 nm. The H_2O_2 concentration was determined based on the method described by Bu *et al.*[22] Approximately 0.1 g of tissue sample was homogenized in 1 mL of ice-cold acetone and centrifuged at 3000*g* for 10 minutes. 0.1 mL of a 5% (w/v) titanium sulfate solution and 0.2 mL of concentrated ammonia solution were added to precipitate the peroxide–titanium complex. The mixture was centrifuged at 3000*g* for 10 minutes. The pellet was then dissolved in 5 mL of 2 M sulfuric acid, and the absorbance of the solution was measured at

410 nm. An analysis of total phenolic contents (TPC) of the extracts was conducted using Folin–Ciocalteu's phenol reagent.[23] The results were expressed as catechin equivalent in milligrams per gram of extract.

Following transcriptome sequencing, we annotated the identified genes, discovered novel genes and conducted a differential gene expression analysis in accordance with the protocols established by Ashraf et al.[17] In detail read alignment to C. tinctorius genome was done by HISAT2 and subsequent transcript assembly and novel gene identification were done by StringTie software (version 2.2.1). Functional annotation of the newly found transcripts was done via comparison against publicly available databases using the DIAMOND (version 2.0.15). The raw transcriptome sequencing data are available in Sequence Read Archive database (https://www.ncbi.nlm.nih.gov/, accessed on 1 September 2025) under accession no. PRJNA1152733.

2.4. Statistical analysis

Statistical analysis was performed using one-way analysis of variance (ANOVA) and treatment means were compared using Tukey's Honestly Significant Difference (HSD) test at 5% significance level. The data were analyzed using Statistics 8.01, and with the help of R-Studio software, the analytical and visualization attributes were utilized for additional computations.

3. Results and discussion

3.1. Characterization of doped nanoparticles

The morphological aspects of the prepared nanocomposite were determined using TEM, which indicated the presence of nano-needles (NN) along with the heterogeneous particles (spherical and rods) attached at their roots. This validated the successful incorporation of the dopant (Se) with CeO_2/Fe_3O_4. Fig. 2A presents the high-resolution image of the distinct heterostructure between Se, Fe_3O_4 and CeO_2 displaying three complementing lattice fringe spacings (d) of 0.305, 0.333 and 0.318 nm. The latter two values correspond to the Miller plane (222) for Fe_3O_4 and (111) for CeO_2, consistent with literature values.[24,25] Elemental mapping via XRD (Fig. 2C) revealed peaks for FeKα1, OKα, CeLα1, and SeLα1_2, confirming the presence of Fe, Ce, O, and Se in the nanocomposite, a finding supported by previous work of Narm et al.[26] The structural properties were further analyzed by XRD (Fig. 2C). The diffractogram showed peaks at 28.51°, 33.12° (assigned to the 111 plane of CeO_2) and 56.39°, while peaks at 47.51° (222) and 76.44° indicated the presence of Fe_3O_4, confirming an uneven distribution of Fe in the lettuce as reported by Li et al.[27] Peaks at 59.05° and 69.45° were attributed to Se doping as confirmed by the previously Fuziki et al.[28]

The zeta potential of synthesized NPs was comparable to the previously reported values in the water (−19.5) and in medium (−20.2) (Fig. 2D). The NPs exhibited less negative values in water than in medium used, indicating a stronger repulsive force between particles. This prevents aggregation, favors greater electrostatic interactions, and enhances the stability of the material in the medium, consistent with other studies.[29,30]

XPS was used to examine the chemical states of Ce, Fe and Se within the NPs. The Ce (3d) spectrum showed peaks at 881, 883, 896, and 898 eV corresponding to the Ce^{3+} and the peaks at 895 and 918 eV, correspond to Ce^{4+} (Fig. 2E). The results indicate that Ce^{4+} was reduced to Ce^{3+}, creating numerous oxygen vacancies that enhance the composites' traits.[31] The Fe 2p spectrum displayed conventional peaks at 710 eV (Fe $2p_{3/2}$) and 725 eV (Fe $2p_{1/2}$) consistent with the Fe_3O_4 as reported by Boda et al.[32] and Liu et al.[33] Similarly, Se (3d) spectrum showed peaks at 58.5 and 63 eV, confirming its incorporation into the composite and its role in the reduction process, which further promotes oxygen vacancy formation.[34] Collectively, these characterization analyses confirm the successful synthesis of the intended nanomaterial.

3.2. Secondary metabolite accumulation and biomass attributes of culture cells

Selenium-doped $CeO_2@Fe_3O_4$ NPs significantly induce the chlorogenic acids (CGAs) biosynthesis in C. tinctorius cells (SI S1), a finding consistent with our previous study of Ashraf et al.[17] A significant increase in fresh and dry biomass of cells of safflower cells was evident following the treatment with different doses of these NPs (Fig. 3A and B). The application of 15 mg L^{-1} Se-doped $CeO_2@Fe_3O_4$ NPs significantly improved the fresh biomass of cells (128%) and dry biomass of cells (128%) compared with the control group (0 mg L^{-1}). While increasing the NPs dosage generally promoted a linear increase in biomass, the highest dose (20 mg L^{-1} T_4 group) caused a reduction of fresh biomass of cells (13.5%) and dry biomass of cells (13.3%) compared to the optimal T_3 group (15 mg L^{-1}). This research extends beyond C. tinctorius and offers potential for synthesizing novel secondary metabolites in other valuable medicinal species. The production of these important compounds is regulated by adding extrinsic biotic or abiotic elicitors and growth regulators, though this can also affect cellular integrity.[36] A comparable variation in the synthesis and release of secondary metabolites has been observed in two species of Zingiber officinale.[37] For instance, Se doped $CeO_2@$-Fe_3O_4 nanoparticles trigger a plant defense response. This necessitates that plants rapidly scavenge reactive oxygen species (ROS) by increasing enzymatic antioxidants activity.

The synergistic interaction of Se dopped $CeO_2@Fe_3O_4$ NPs, and their influence on nutrient availability and cellular processes leads to a significant enhancement in both fresh and dry biomass. The metallic NPs acted as a potential nanozyme, which catalytically neutralise excessive ROS related molecules such as hydrogen peroxide and superoxide anions, reducing the oxidative damage to cellular membranes and biomolecules and subsequently leading to healthier cell division and biomass accumulation.[13,17,36] The data indicated that the application of metallic nanomaterials significantly altered cell growth in dose–dependent ways, as well as metabolomics profiling and molecular pathways in several plant species, including Brassica juncea,[38] Triticum aestivum,[39] Melissa officinalis,[40] peppermint,[41] and sorghum.[42] Furthermore, numerous factors, such as the
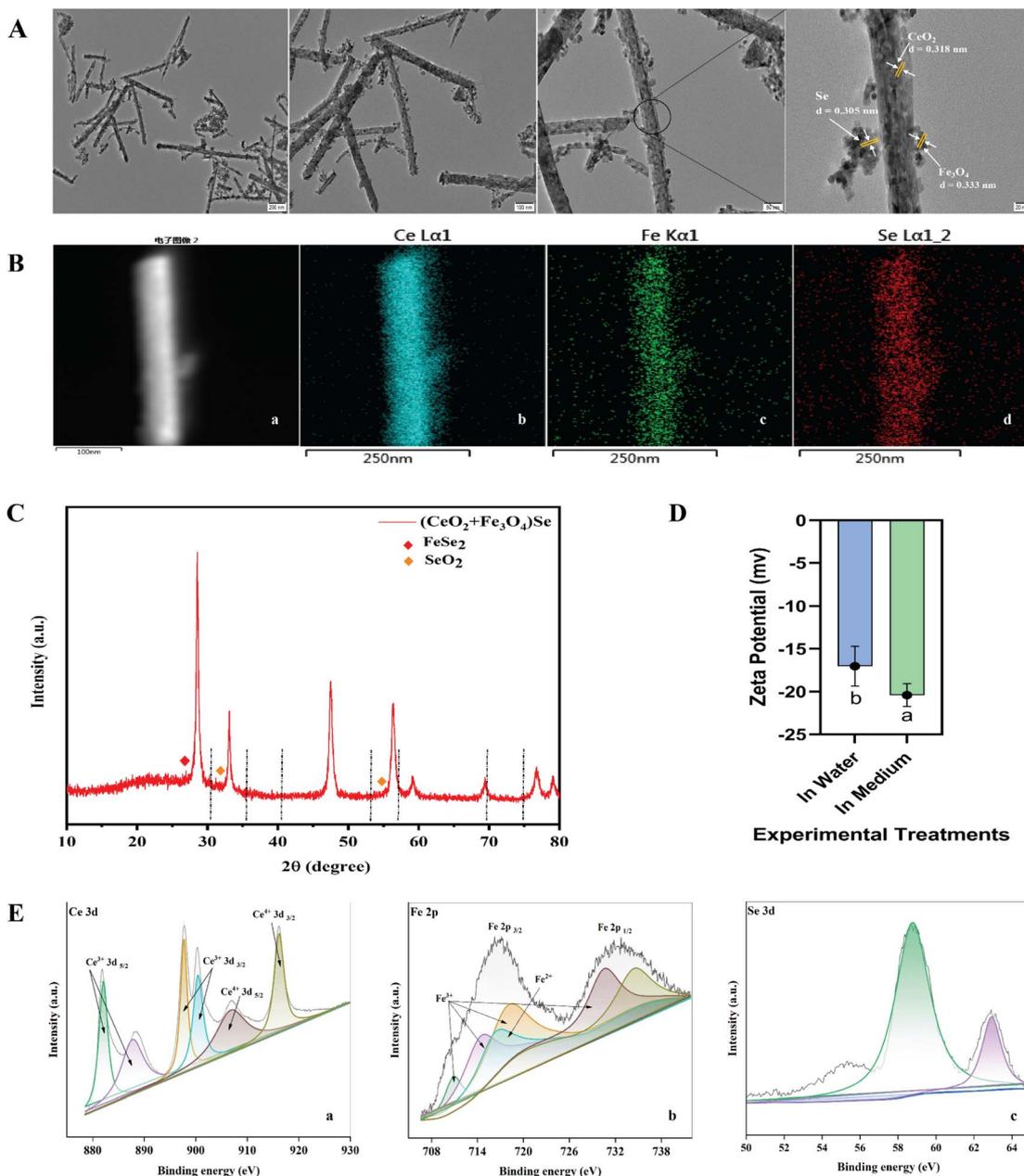
Fig. 2 Characterization of synthesized NPs (A); high-resolution transmission electron microscopy (HRTEM) analysis of NPs at various resolutions (B); (a) EDS (TEM) of aggregated NPs, (b) EDS (TEM) of Ce, (c) EDS (TEM) of Fe, (d) EDS (TEM) of Se, (C); X-ray analysis for elemental status on XRD pattern of $(CeO_2 + Fe_3O_4)$ Se, (D); zeta potential (mv), (E); XPS spectra of NPs; spectrum of $(CeO_2 + Fe_3O_4)$ Se.

synthesis process,[43] appropriate concentration, and specific biological systems involved, result in varying beneficial effects and cellular toxicity of nanoproducts.[44] Convincing evidence indicates that the absorption of metallic NPs and their subsequent metabolism differ from those in control group. The presence of selenium (Se) and iron (Fe) ions facilitates enhanced ATP production and carbon fixation, which may contribute to the improved growth and increased biomass observed in the cells.[17,36] An optimum concentration of NPs significantly enhanced the growth attributes; however, beyond a reference dose, cellular growth was significantly affected, as mentioned in the prior studies.[45,46]

3.3. Chlorophyll and soluble protein contents

The application of Se-doped $CeO_2@Fe_3O_4$ NPs in safflower cell suspension culture significantly improved the pigments and soluble protein contents (Fig. 3C–F). Increasing the concentration of the NPs resulted in a linear rise in the chlorophyll contents. The T_3 treatments group exhibited a maximum increase in the chlorophyll a (49.8%), chlorophyll b (163%), total chlorophyll contents (76.0%) and soluble sugars (172%). When combined with the soluble protein and chlorophyll data, the measurement of enzymatic antioxidant activity provides an integrated view of cellular adaptive strategies, stress resistance and overall metabolic performance. The addition of various
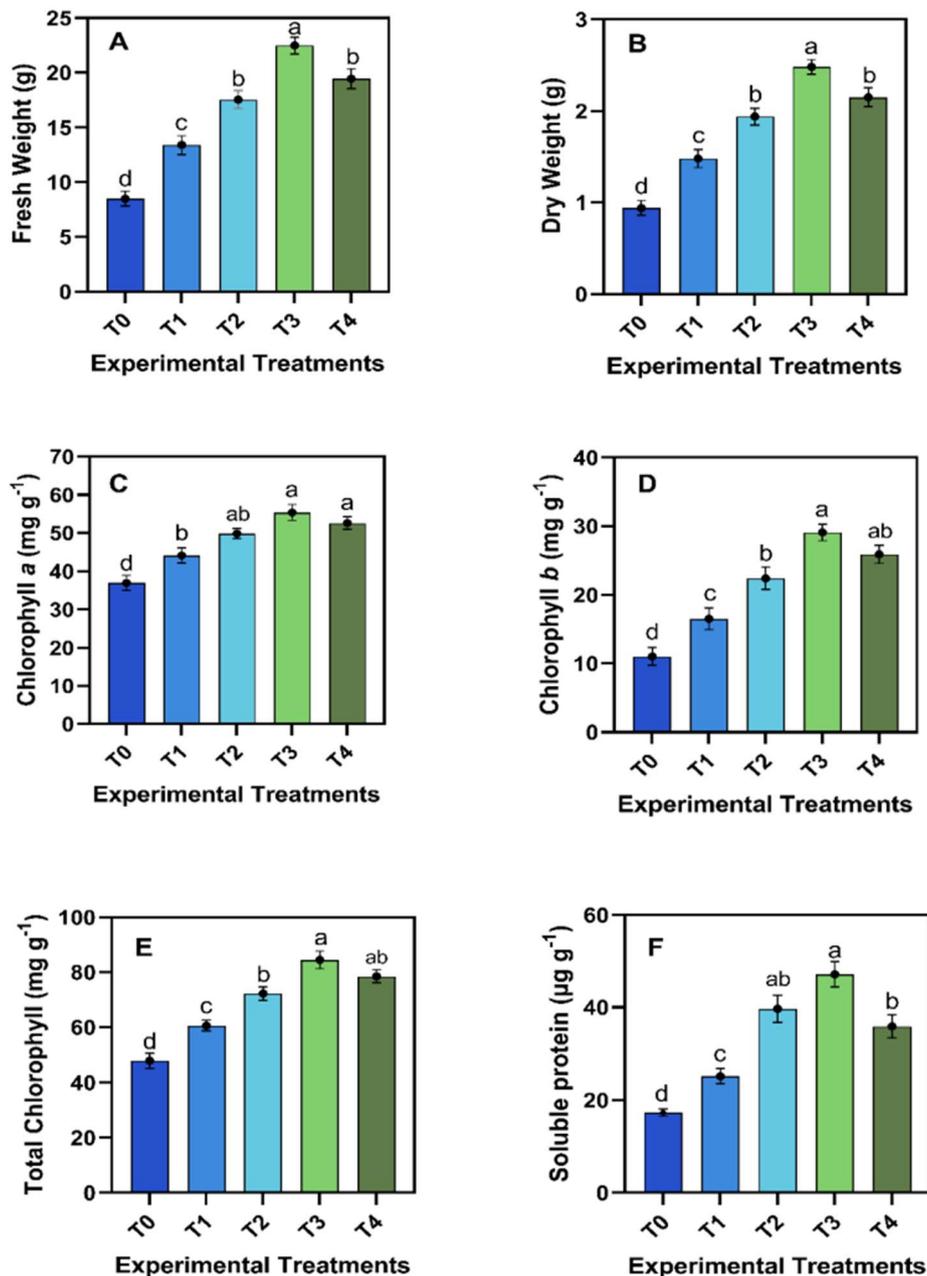
Fig. 3 Effects of various doses of Se doped $CeO_2@Fe_3O_4$ (mg L^{-1}) NPs on (A) fresh weight of cells; (B) dry weight of cells; (C–E) chlorophyll (a, b, Total) contents; (F) soluble protein of safflower in cell suspension culture. Results were expressed as mean values ± standard deviation ($n = 3$). Bars with different letters have values indicating significant differences at the 5% level using Tukey's honestly significant difference test. [$T_0 = 0$ mg L^{-1}; $T_1 = 5$ mg L^{-1}; $T_2 = 10$ mg L^{-1}; $T_3 = 15$ mg L^{-1}; $T_4 = 20$ mg L^{-1}].

concentrations Se-doped $CeO_2@Fe_3O_4$ improved the chlorophyll pigment levels and increased the accumulation of soluble protein contents (Fig. 3). This enhancement in chlorophyll contents within safflower cell suspension culture can be attributed to several key mechanisms. The doping of selenium, an essential micronutrient, into $CeO_2@Fe_3O_4$ NPs offers a supplemental source of this element, which acts as a cofactor for enzymes that regulate chlorophyll synthesis, as it plays a crucial role in enhancing ribosomal activity, which ultimately results in the chlorophyll biosynthetic pathway.[17,36] Its presence may also upregulate genes associated with chlorophyll

production.[47] Furthermore, the unique physico-chemical traits of NPs, such as high surface area and reactivity, facilitate effective delivery and uptake of nutrients into the cells.[48] The improved chlorophyll contents might be due to the scavenging activity of ROS through the superoxide dismutase (SOD)-mimetic activity of CeO_2 and the catalase (CAT)-mimetic activity of Fe_3O_4, which are the integral components of synthesized NPs.[36] Nanoparticles function as effective nano-carriers, facilitating the controlled release of selenium. This approach prevents the rapid depletion of selenium and ensures a consistent supply to plant cells.[49,50] The presence of iron oxide
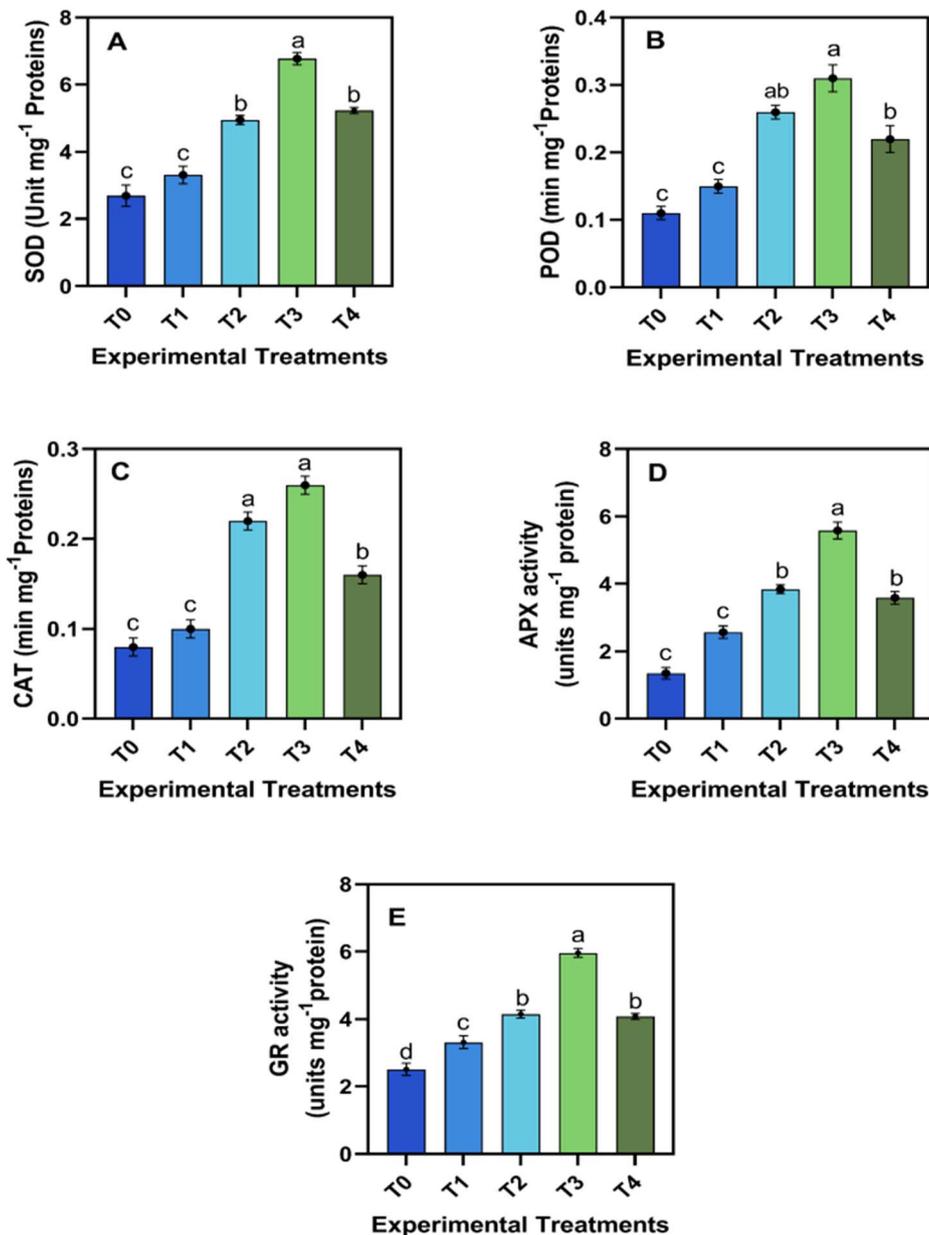
Fig. 4 Effects of various doses of Se doped $CeO_2@Fe_3O_4$ (mg L^{-1}) NPs on the enzymatic antioxidants of safflower cells in suspension culture. [(A) super oxide dismutase activity (SOD); (B) peroxidase activity (POD); (C) catalase activity (CAT); (D) ascorbate peroxidase activity (APX); (E) glutathione reductase activity (GR)]. Results were expressed as mean values $\pm$ standard deviation ($n = 3$). Bars with different letters have values indicating significant differences at the 5% level using Tukey's honestly significant difference test. [$T_0 = 0$ mg L^{-1}; $T_1 = 5$ mg L^{-1}; $T_2 = 10$ mg L^{-1}; $T_3 = 15$ mg L^{-1}; $T_4 = 20$ mg L^{-1}].

in the NPs structure may further aid nutrient transport and uptake, thereby supporting chlorophyll synthesis.[51]

3.4. Enzymatic antioxidants

The enzymatic antioxidant attributes of safflower suspension cells were linearly improved by the application of Se-doped $CeO_2@Fe_3O_4$ NPs (Fig. 4A–E). A linear increase in the enzymatic antioxidants was noticed up to the T_3 treatment group (15 mg L^{-1}); however, the highest concentration (20 mg L^{-1}) of doped NPs caused a decline in all the activities of enzymatic antioxidants. Maximum increase in SOD activity (151%), POD

activity (181%), CAT activity (225%), APX activity (313%) and GR activity (137%) was observed in T_3 treatment group, compared with control. Measuring antioxidant profiles, ROS attributes and total phenolics following the assessment of enzymatic antioxidants in plant cell suspension cultures provides a deeper insight into cellular redox state and defense capabilities. These collective parameters elucidate plant cellular response to oxidative stress, enabling researchers to adjust culture conditions for improved growth, enhanced metabolite production, and better stress resistance. Furthermore, the addition of Se-doped $CeO_2@Fe_3O_4$ to the culture media significantly
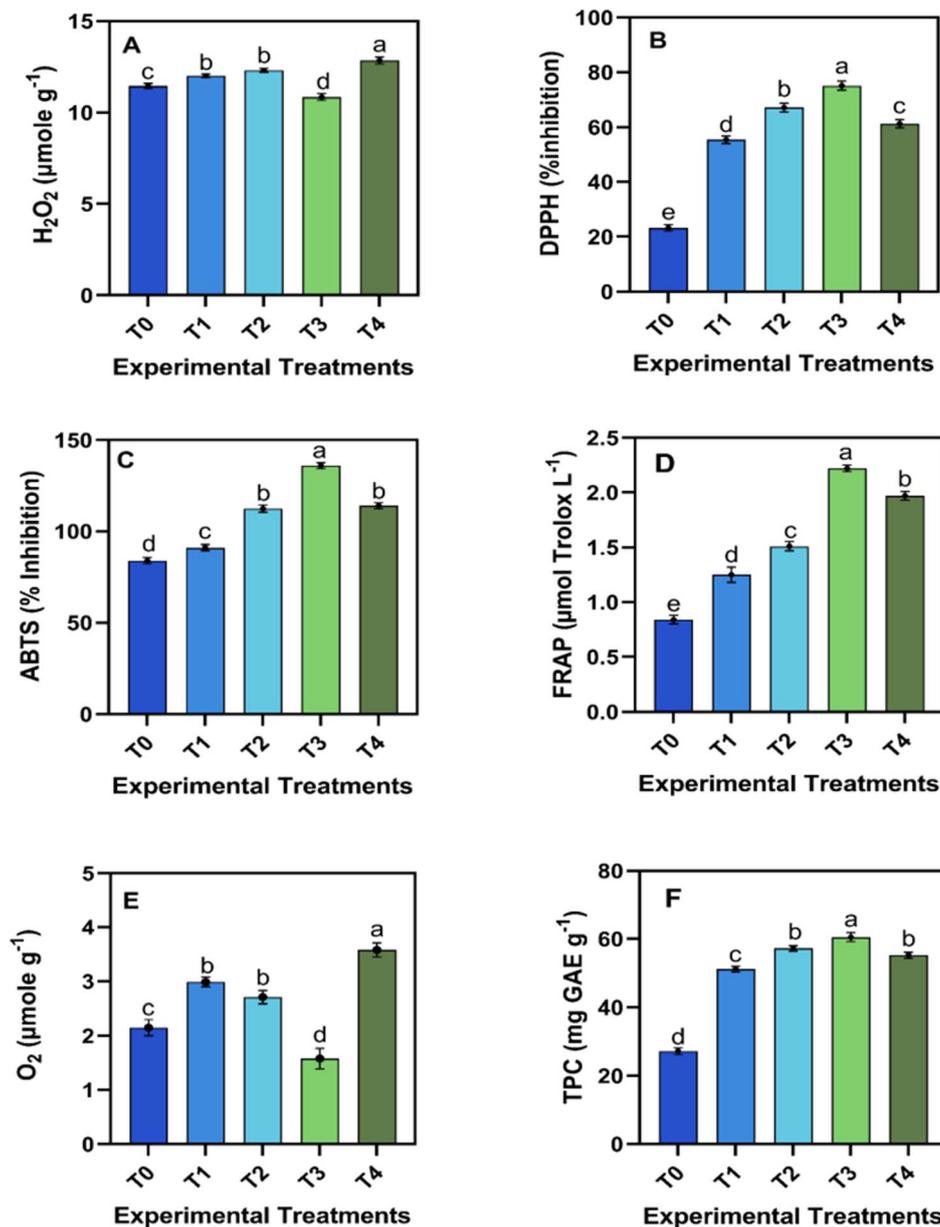
Fig. 5 Effects of various doses of Se doped $CeO_2@Fe_3O_4$ (mg L^{-1}) NPs on antioxidant profile, ROS related and total phenolics contents of safflower in cells suspension culture. [(A) hydrogen peroxide H_2O_2 activity; (B) DPPH scavenging activity; (C) FRAP activity; (D) ABTS activity; (E) O_2 contents; (F) total phenolic contents] in safflower in suspension culture. Results were expressed as mean values $\pm$ standard deviation ($n = 3$). Bars with different letters have values indicating significant differences at the 5% level using Tukey's honestly significant difference test. [$T_0 = 0$ mg L^{-1}; $T_1 = 5$ mg L^{-1}; $T_2 = 10$ mg L^{-1}; $T_3 = 15$ mg L^{-1}; $T_4 = 20$ mg L^{-1}].

enhanced the enzymatic antioxidative activities compared to the control group (Fig. 4). The maximum expression of SOD and peroxidase (POD) activities was observed in the cells cultivated at 15 mg L^{-1} of NPs. The SOD is a key antioxidant metalloprotein enzyme in plants that catalyses the conversion of SOD free radicals into hydrogen peroxide.[52] Its activation helps to safeguard plant cells from oxidative stress under adverse conditions.[53,54] Moreover, the application of metallic NPs in a dose–dependent manner is considered as a potential component affecting the enzymatic antioxidant profile in both *in vitro* and *in vivo* systems.[55] The possible reason for the improved enzymatic antioxidant activities might be due to the

Se that helps to integrate seleno-proteins,[17] which effectively improve the glutathione cycle, scavenging the ROS production through the ascorbate–glutathione pathway.

3.5. Antioxidant profile, ROS attributes and total phenolics

The application of Se-doped $CeO_2@Fe_3O_4$ NPs significantly improved the antioxidant profile and total phenolic contents while decreasing the ROS related attributes in cultured cells (Fig. 5A–F). Various rates of these NPs induced a linear increase in the antioxidant activity, as measured by ABTS, DPPH and FRAP assays. A maximum increase in the percent inhibition and
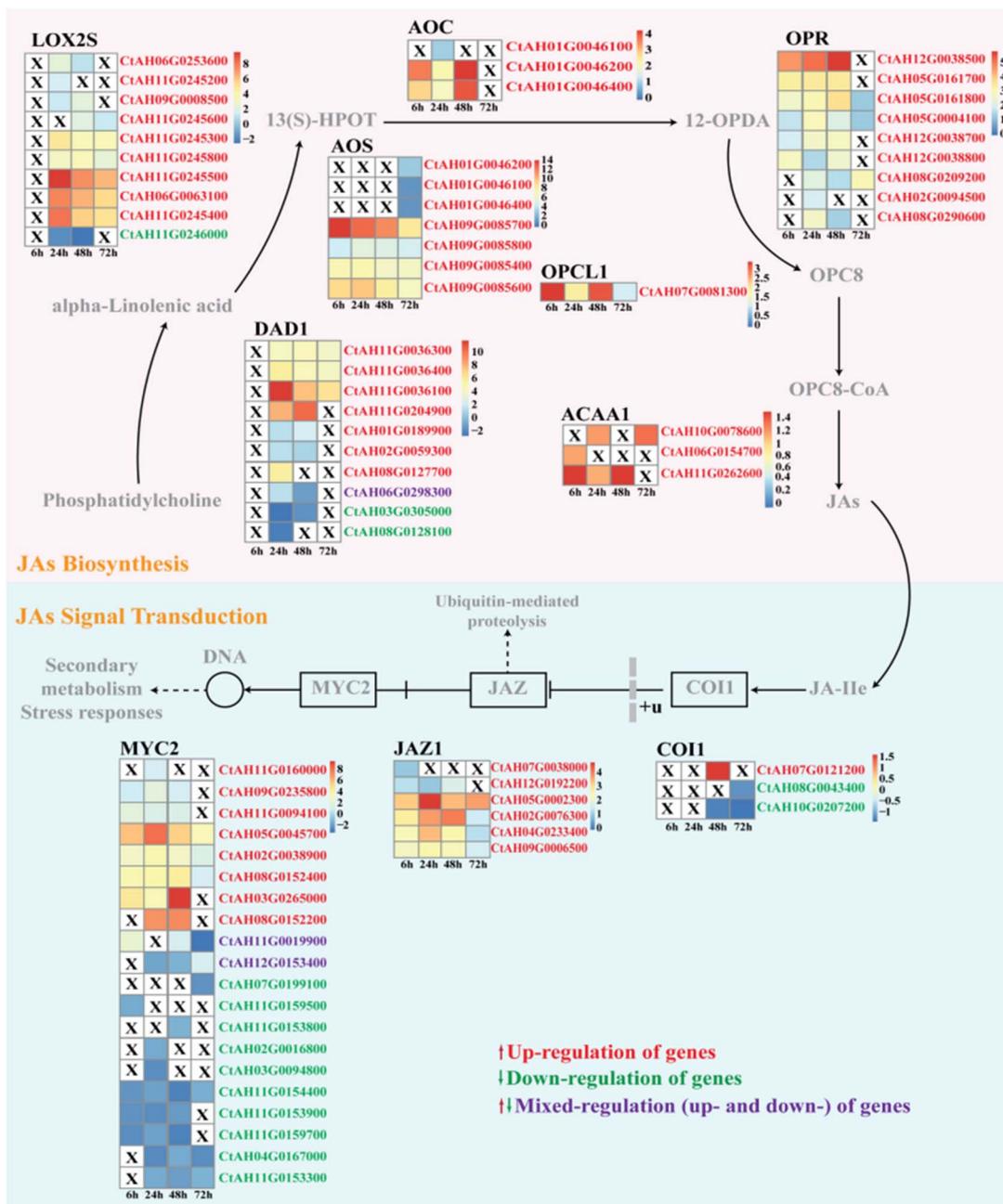
Fig. 6 Differences in jasmonate (JAs) biosynthesis and it signaling pathways at the transcriptional level. The relative fold changes in gene expression between the NPs-treated and the control groups at various time points (6 h, 24 h, 48 h, and 72 h) are shown by the colored rectangles. The "X" within the gene family denotes the gene that is either unexpressed or not very differentially expressed at a particular time. The hypothetical pathways represented by the dashed arrow have not been completely verified.

a 122% improvement in total phenolics were observed in the T_3 treatment group of safflower cell suspension culture compared to the control group. The T_3 treatment group exhibited reduced levels of hydrogen peroxide (5.15%) and reactive oxygen (26.5%) compared to the control group (0 mg L^{-1}). However, at the highest level of these NPs caused a decrease in antioxidant profile and total phenolics, alongside an increase in ROS-related parameters. Transcriptional analysis integrates molecular data with physio-biochemical findings to decode plant cellular networks. This enables the refinement of culture techniques to enhance metabolite production and improve stress resilience. The unregulated release of ROS during plant morphogenesis decreases cell redifferentiation and dedifferentiation. This process can directly or indirectly lead to the production of toxic substances.[56] To mitigate such oxidative stress, plants synthesize tissue-specific stress enzymes.[57] According to Abbasi *et al.*,[56] these enzymes form an integrated defense system that protects plant tissues from mono-oxygen
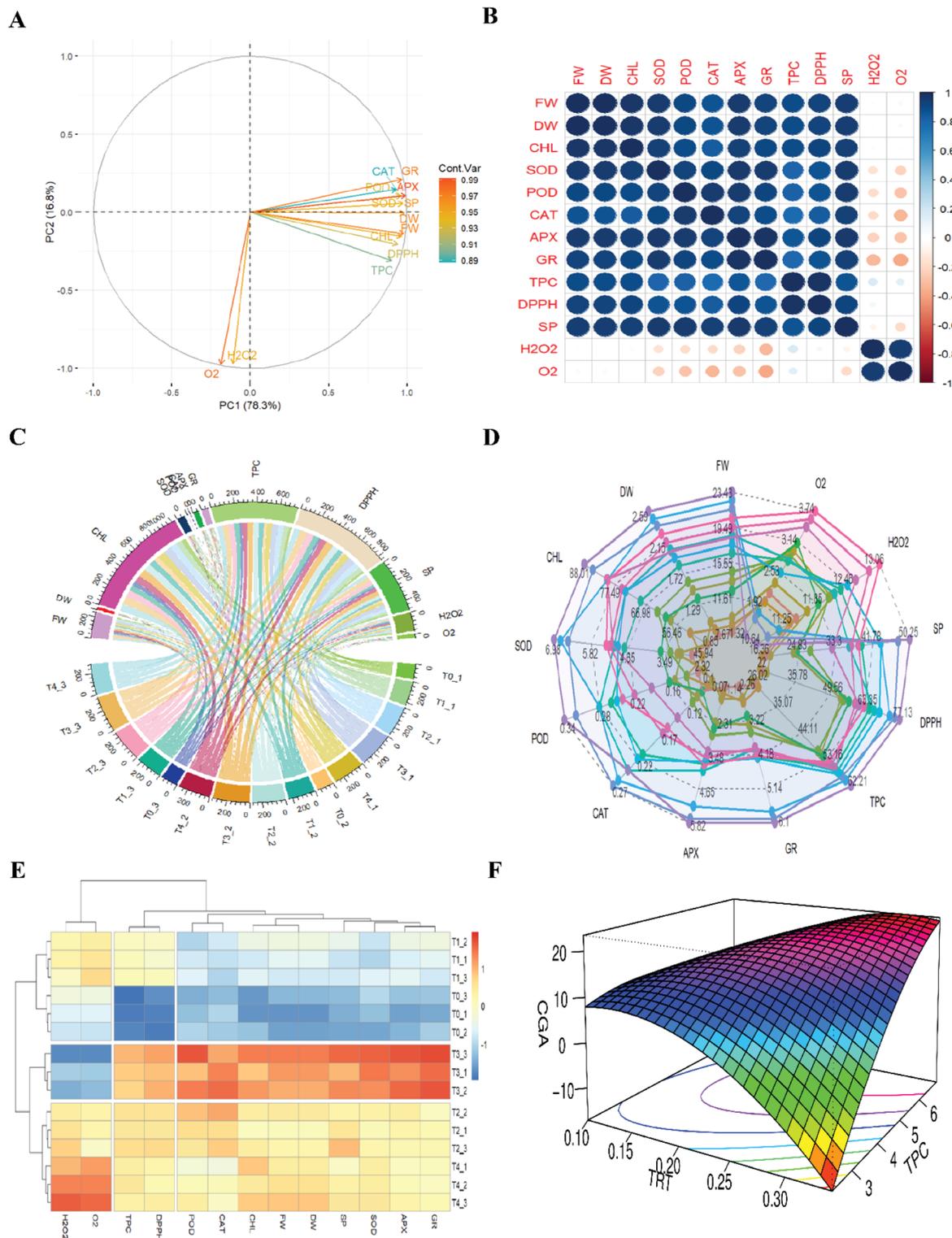
Fig. 7 Multivariate analysis of growth, physiological and biochemical parameters under various levels of Se doped CeO_2@Fe_3O_4 NPs treatment conditions: (A) principal component analysis (PCA) biplot; (B) correlation matrix among measured parameters; (C) chord plot between treatments and variables; (D) redar analysis across treatment means; (E) heatmap of measured parameters, and (F) 3D response surface model between key variables; $T_0 = 0$ mg L^{-1}; $T_1 = 5$ mg L^{-1}; $T_2 = 10$ mg L^{-1}; $T_3 = 15$ mg L^{-1}; $T_4 = 20$ mg L^{-1}; FW = fresh weight of cells; DW = dry weight of cells; CHL = total chlorophyl contents; DPPH = (2,2-diphenyl-1-picrylhydrazyl)assay; SP = soluble protein contents; SOD = superoxide dismutase activity; POD = peroxidase activity; APX = ascorbate peroxidase activity; GR = glutathione reductase activity; TPC = total phenolics contents; H_2O_2 = hydrogen peroxide activity and O_2 = reactive oxygen contents.
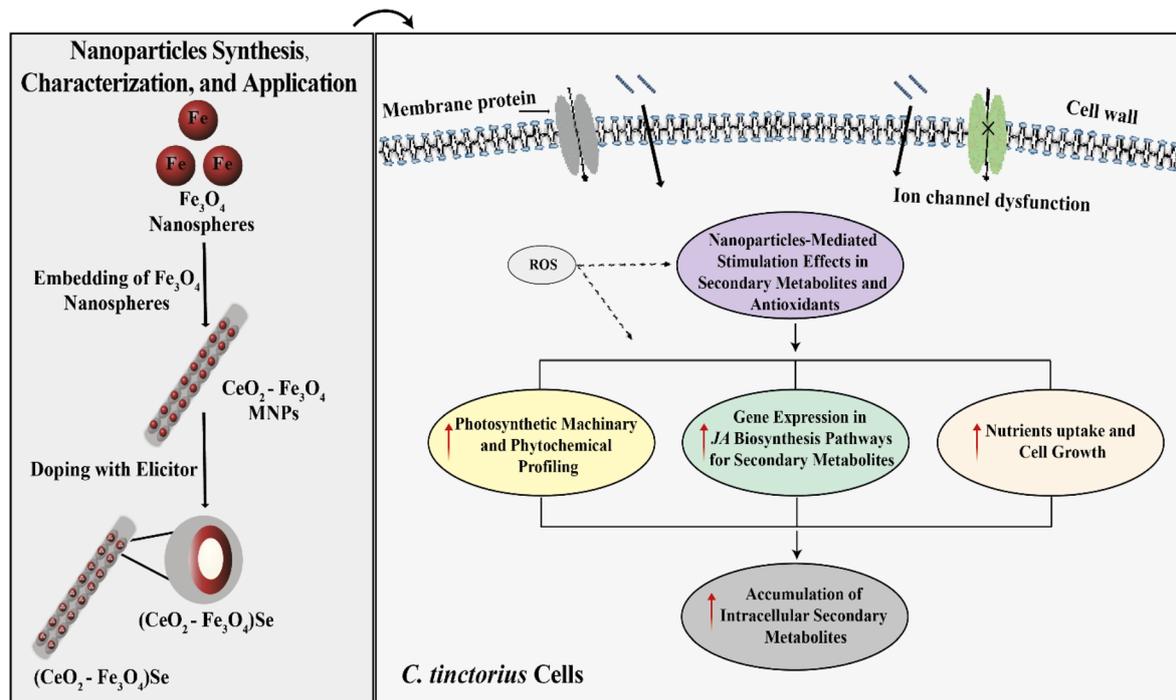
Fig. 8 The application of Se-doped CeO$_2$@Fe$_3$O$_4$ NPs to *C. tinctorius* cells initiates a multi-faceted mechanism. The NPs interact with the cell membrane, resulting in reduced production of reactive oxygen species (ROS), and consequently minimal disruption to ion channels. This interaction further stimulates enhanced nutrient uptake and promotes cell growth. Simultaneously, the NPs alter the expression levels of genes in the jasmonic acid (JA) biosynthesis pathways. As a result, the photosynthetic machinery is stimulated, the phytochemical profiling is improved, and secondary metabolites including antioxidants accumulate within intracellular compartments. This mechanism underscores the significant role of NPs in stimulating secondary metabolism and boosting overall cellular productivity.

derived species. The multivariate analysis in this experiment indicates that exposing suspended cells to various metallic NPs enhanced the synthesis of these stress enzymes, compared to the control. This enhancement improved the phenolic contents and antioxidative profile of safflower cells (Fig. 7). Numerous studies on enzymatic antioxidants report similar findings on various species, including *Prunus* and *Solanum*.[58] Additionally, callus cultures of *Acanthophyllum sordidum* have been shown to produce only small quantities of these enzymes during dedifferentiation, with a gradual increase during redifferentiation.[59–61] At the transcriptomic level, exposure to metallic NPs usually leads to upregulations of the expression of important endogenous antioxidant genes and stress responsive transcription factors, as well as the modulation of genes involved in phytohormone signalling and nutrient assimilation.[62] The production and role of these enzymatic antioxidants have also been demonstrated in many other plant species.[63,64] During adverse conditions, singlet free radicals are generated in the plant cells, which can react with macromolecules and ultimately inhibit the growth of different plant tissues.[65,66] In response to these highly reactive singlet radicles, certain plant tissues produce polyphenolics to scavenge free radicals for use in subsequent processes.[67,68] Collectively, the dual response, such as scavenging ROS and stimulating defense pathways might be the possible reason for increased phenolic accumulation in safflower (Fig. 8).

3.6. Transcriptional analysis

The alpha-linolenic acid metabolism pathway produces endogenous jasmonate, which is crucial for responding to environmental stress. Analysis of the endogenous jasmonate biosynthesis pathways identified 108 differentially expressed genes (DEGs) from 14 gene families, all showing considerable up-regulation expression. Among these, the 13-lipoxygenase (*LOX2S*) and phospholipase A1 (*DAD1*) families contained the maximum number of DEGs (10 each), followed by 12-oxophytodienoate reductase (*OPR*) and hydroperoxide dehydratase (*AOS*) with 9 and 7 DEGs, respectively (Fig. 6). The jasmonate signalling pathway also includes coronatine-insensitive protein 1 (*COI-1*), jasmonate ZIM domain-containing protein (*JAZ*) and basic helix-loop-helix *MYC2* (MYC2). Griffiths,[35] reported that *JAZ* and *MYC2* regulate the secondary metabolites by affecting the promoter regions of transcription factors or structural genes. In this study, 29 DEGs were identified in the jasmonate signaling pathway. Eight DEGs from the *MYC2* family, six from the *JAZ* family, and one from the *COI1* family were up-regulated. In contrast, the expression of the ten other DEGs in *MYC2* family and two in the *COI1* family was decreased. Only two DEGs in the *MYC2* family showed mixed expression at different time points (6 h, 24 h, 48 h, and 72 h) following treatment with Se-doped CeO$_2$@Fe$_3$O$_4$ NPs. Consequently, in *C. tinctorius* cells, Se-doped NPs significantly increased the jasmonate production and its signaling pathways. These pathways upregulate the

genes responsible for the antioxidant's biosynthesis. Therefore, the enhanced jasmonate levels resulting from the treatment with Se-doped NPs act as a signal that primes the plant cells to increase their defense systems by inducing these produced antioxidative compounds. Multivariate analyses are essential techniques for understanding the complex experimental data in detail and for optimizing variables across experiments. Adhering to scientific standards through these methods strengthens the integrity of the results, making the conclusions more relevant for practical applications.

3.7. Multivariate and response surface methodology analysis

To evaluate the relationship between measured attributes under the influence of various dosages of Se-doped CeO_2@Fe_3O_4 NPs, multivariate analyses were depicted in Fig. 7A–F. The principal component analysis (PCA) plot shows a total variability of 78.30% of PC1 and 16.80% of PC2. The T_3 treatments cluster associated with a higher NPs concentration (dose level ~15 mg L^{-1}), groups enzymatic antioxidants that are part of the plant's defense mechanism. In contrast, the cluster T_4 treatment group (dose level ~20 mg L^{-1}), primarily affects total chlorophyll content, and fresh and dry cell weights in safflower suspension culture (Fig. 7A). Correlation analysis showed significant positive correlations among biomass, chlorophyll and phenolics and antioxidative profiles. Conversely, the ROS related attributes showed a significant negative correlation with all measured attributes (Fig. 7B). Similarly, a chord diagram illustrates the association between the treatment and attributes; the size of the arc is proportional to the importance of each flow. Treatments T_0 (control) demonstrates a relatively smaller influence compared to the other treatments (T_2 to T_4) (Fig. 7C). Redar analysis depicts that the outermost lines represent treatment eliciting the higher response, while the inner lines correspond to lower increase across parameters. The results indicate that specific levels of NPs can significantly increase antioxidant enzyme activity and secondary metabolite accumulation without inducing oxidative damage (Fig. 7D). Heatmap shows the strength and type of association between measured variables and the treatments. The treatment T_3, showed a strong positive correlation with SOD, APX and GR, whereas the control (T_0 group) is negatively correlated with DPPH, GR, and other measured attributes (Fig. 7E). Response surface methodology analysis indicates that an increase in total phenolics contents (TPC) corresponds to increase in chlorogenic acid (CGA) levels, demonstrating a significant correlation between phenolic compound biosynthesis and CGA production (Fig. 7F). Contour lines at the base identify optimal regions for achieving maximum CGA content at moderate to high TPC and treatment levels. This highlights how elevating phenolic content through optimized treatment can enhance CGA biosynthesis, highlighting the potential of elicitor-based approaches to boost the antioxidative and therapeutic properties of safflower cells. The correlation matrix indicates that TPC, DPPH and enzymatic activities are strongly positively correlated with each other. In contrast, reactive oxygen species (H_2O_2 and O_2^-) show an inverse correlation, indicating a reduction of oxidative stress by the application of NPs treatment. These

analyses showed that Se doped CeO_2@Fe_3O_4 NPs enhance the antioxidative profile in combined treatment by up-regulating enzymatic and nonenzymatic antioxidants, suppressing ROS and promoting the production of secondary metabolites in safflower cells. These findings directly link the action of NPS to the stimulation of secondary metabolism and an increase in overall cell productivity (Fig. 7). We demonstrate that these nano environments can enhance safflower biomass and sustain this enhancement over time. Furthermore, the use of synthesized nanomaterials as elicitors was validated through their application in an *in vitro* plant culture system. In summary, this study presents a novel approach for increasing the yield of enzymatic antioxidants from medicinal plants in controlled culture systems, with significant potential implications for the pharmaceutical industry.

4. Conclusion

The optimal concentration of Se-doped CeO_2@Fe_3O_4 NPs was found to enhance cell growth and significantly modulate antioxidative and phenolic contents in safflower cell suspension cultures. Specifically, supplementation of the culture medium with 15 mg L^{-1} of these NPs promoted antioxidative defense by scavenging reactive oxygen species (ROS), resulting in the upregulation of antioxidative enzyme activities. This process highlights the adaptive response involving jasmonate (JAs) production and its signaling pathway in callus cultures, which aids in preventing oxidative stress and maintaining cellular homeostasis. The application of Se-doped CeO_2@Fe_3O_4 NPs thus presents an innovative methodology for enhancing antioxidant synthesis in plant cell cultures and is recommended for the production of valuable plant metabolites in various *in vitro* cell suspension systems. More in-depth studies on this doped nano-elicitation approach in bioreactors and its economic viability for the industrial production of valuable safflower metabolites to develop cost-effective magnetic recovery for large-scale use are recommended. Moreover, the integration of ionic controls and dissolution assays, with emphasis on elucidating cellular internalization pathways (such as endocytosis or pore entry) and intracellular fate (including persistence as particles, dissolution into ions, or transformation), is essential to distinguish nanoparticle-specific effects from ion-mediated effects in future studies.

Author contributions

Author statement K. A., A. M., M. G.: data analysis, investigation, methodology, original draft, conceptualization and formal analysis; K. A.,Y. L., S. G., A. S.: experimental part, investigation and methodology; K. A., M. A., M. M.,; data curation; K. A., Y. L., N. Y. R.: writing – review & editing; K. A., A. S., A. M.: conceptualization, K. A., M. G., A. M. Q. Z.: writing – review & editing, M. G., A. S., Q. Z.: supervision M. G., A. M.

Conflicts of interest

The authors declare no competing interests.

Data availability

Acknowledgements

References

1 F. Berti, E. M. Tamburello and C. Forzato, *Molecules*, 2025, **30**, 1259.

2 C. Kurt, M. T. Altaf, W. Liaqat, M. A. Nadeem, A. N. Çil and F. S. Baloch, *Foods*, 2025, **14**, 264.

3 V. Mani, K. Natesan, J. W. Choi, M. K. Swamy, and B. M. K. Vasamsetti, in *Phytochemical Genomics: Plant Metabolomics and Medicinal Plant Genomics*, Singapore, Springer Nature Singapore, 2023, pp 127–143.

4 K. Ashraf, Q. Zaman, W. Tang, P. Jiang, X. Wan, K. Yuri, A. Mohsin and G. Meijin, *Front. Plant Sci.*, 2025, **16**, 1679901.

5 F. Abdulhafiz, A. Mohammed, M. F. H. Reduan, Z. A. Kari, L. S. Wei and K. W. Goh, *Arabian J. Chem.*, 2022, **15**, 104161.

6 V. A. Bapat, P. B. Kavi Kishor, N. Jalaja, S. M. Jain and S. Penna, *Agronomy*, 2023, **13**, 858.

7 M. A. Fazili, I. Bashir, M. Ahmad, U. Yaqoob and S. N. Geelani, *Bull. Natl. Res. Cent.*, 2022, **46**, 35.

8 G. D. Vyavahare, R. R. Patil and J. H. Park, *Plant Growth Regul.*, 2025, **1**, 28.

9 M. Darbahani, M. R. Ghiyasi and M. Rahaie, *Phytochem. Rev.*, 2024, 1–25.

10 P. K. Sahu, K. Jayalakshmi, J. Tilgam, A. Gupta, Y. Nagaraju, A. Kumar and M. V. S. Rajawat, *Front. Plant Sci.*, 2022, **13**, 1042936.

11 R. K. Singhal, S. Fahad, P. Kumar, P. Choyal, T. Javed, D. Jinger and T. Nawaz, *Plant Growth Regul.*, 2023, **100**(2), 237–265.

12 M. Darbahani, M. R. Ghiyasi and M. Rahaie, *Phytochem. Rev.*, 2025, **24**, 3179.

13 H. Sun, A. Sohail, A. Shah, Z. Liaqat and M. Gul, *Phytopharmacol. Res. J.*, 2025, **4**(2), 28–42.

14 R. Yousaf, M. A. Khan, A. Raza, Ambreen, H. Ali, H. Darwish, K. Alharbi, N. A. T. Al Kashgry and A. Noureldeen, *Plant Cell Tissue Organ Cult.*, 2025, **160**(2), 27.

15 L. Wang, F. Shafiq, Z. Ding and Y. He, *Front. Plant Sci.*, 2025, **16**, 1714617.

16 M. Guo, H. Lv, H. Chen, S. Dong, J. Zhang, W. Liu and H. Luo, *Chin. Herb. Med.*, 2024, **16**(1), 13–26.

17 K. Ashraf, Z. Liu, Q. uz Zaman, M. Arshad, W. Q. Zaman, A. Shan, J. Yu, T. Rehman, Y. Zhuang, M. Guo and A. Mohsin, *Chem. Eng. J.*, 2025, **503**, 159705.

18 Z. Liu, X. Zhu, A. Mohsin, H. Sun, L. Du, Z. Yin and M. Guo, *Int. J. Mol. Sci.*, 2024, **25**(5), 2710.

19 C. Peng, F. Gao, H. Wang, H. Shen and L. Yang, Physiological and Biochemical Traits in Korean Pine Somatic Embryogenesis, *Forests*, 2020, **11**(5), 577.

20 S. Sethi, A. Joshi, B. Arora, A. Bhowmik, R. Sharma and P. Kumar, *Eur. Food Res. Technol.*, 2020, **246**, 591–598.

21 B. Zhao, X. Wang, H. Liu, C. Lv and J. Lu, *Int. J. Biol. Macromol.*, 2020, **150**, 737–745.

22 R. Bu, J. Xie, J. Yu, W. Liao, X. Xiao and J. Lv, *J. Plant Biol.*, 2016, **59**, 247–259.

23 H. H. Orak, M. Karamac and R. Amarowicz, *Oxid. Commun.*, 2015, **38**, 67–76.

24 X. Du, Y. Ding and X. Zhang, *Appl. Surf. Sci.*, 2021, **562**, 150227.

25 D. L. Li, Z. G. Gu, W. Zhang, Y. Kang and J. Zhang, *J. Mater. Chem. A*, 2017, **5**(38), 20126–20130.

26 T. S. Narm, H. Hamidinezhad, Z. Sabouri and M. Darroudi, *Environ. Technol. Innov.*, 2024, **34**, 103617.

27 K. Li, Y. Zhao, C. Song and X. Guo, *Appl. Surf. Sci.*, 2017, **425**, 526–534.

28 M. E. K. Fuziki, R. Brackmann, T. S. Dias, A. M. Tusset, S. Specchia and G. G. Lenzi, *J. Water Process Eng.*, 2021, **42**, 102163.

29 S. O. Oselusi, N. R. Sibuyi, M. Meyer, S. Meyer and A. M. Madiehe, *Mater. Today Sustain.*, 2025, **29**, 101059.

30 A. Maryum, H. Yasmin, Q. Saeed, A. M. Ahmed, S. M. Popescu and F. Ahmad, *J. King Saud Univ. Sci.*, 2024, **36**(5), 103162.

31 T. D. Nguyen, C. T. Dinh and T. O. Do, *Inorg. Chem.*, 2011, **50**, 1309–1320.

32 S. K. V. A. A. Boda, B. Basu and B. Sahoo, *J. Phys. Chem. C*, 2015, **119**, 6539–6555.

33 Q. Liu, L. B. Zhong, Q. B. Zhao, C. Frear and Y. M. Zheng, *ACS Appl. Mater. Interfaces*, 2015, 7, 14573–14583.

34 D. S. Han, B. Batchelor and A. Abdel-Wahab, *Environ. Prog. Sustain. Energy*, 2013, **32**, 84–93.

35 G. Griffiths, *Essays Biochem.*, 2020, **64**, 501–512.

36 P. Golkar, E. Vázquez-Núñez and J. R. Peralta-Videa, *Plants*, 2025, **15**, 46.

37 A. Ghasemzadeh, H. Z. E. Jaafar, A. Rahmat, P. E. M. Wahab and M. R. A. Halim, *Int. J. Mol. Sci.*, 2010, **11**, 3885–3897.

38 N. Handa, S. K. Kohli, A. Sharma, A. K. Thukral, R. Bhardwaj and E. F. Abd_Allah, *Environ. Exp. Bot.*, 2019, **161**, 180–192.

39 M. Safari, Z. Oraghi Ardebili and A. Iranbakhsh, *Acta Physiol. Plant.*, 2018, **40**, 117.

40 A. Babajani, A. Iranbakhsh, Z. Oraghi Ardebili and B. Eslami, *Environ. Sci. Pollut. Res.*, 2019, **26**, 24430–24444.

41 H. Nazerieh, Z. O. Ardebili and A. Iranbakhsh, *Acta Agric. Slov.*, 2018, **111**, 357–368.

42 M. Djanaguiraman, N. Belliraj, S. H. Bossmann and P. V. Prasad, *ACS Omega*, 2018, **3**, 2479–2491.

43 B. Abbasi, J. Iqbal, R. Ahmad, L. Zia, S. Kanwal and T. Mahmood, *Biomolecules*, 2020, **10**, 38.

44 M. Moghanloo, A. Iranbakhsh, M. Ebadi, T. N. Satari and Z. O. Ardebili, *Acta Physiol. Plant.*, 2019, **41**, 1–13.

45 H. F. Alharby, E. M. Metwali, M. P. Fuller and A. Y. Aldhebiani, *Arch. Biol. Sci.*, 2016, **68**, 723–735.

46 R. Javed, B. Yucesan, M. Zia and E. Gurel, *Sugar Tech.*, 2018, **20**, 194–201.

47 A. A. Shah, N. A. Yasin, M. Mudassir, M. Ramzan, I. Hussain, M. H. Siddiqui and R. Kumar, *Environ. Pollut.*, 2022, **307**, 119413.

48 T. Patel, C. Clipstone, U. V. Girija, Z. Ahmad and N. Singh, *Nanomaterials*, 2025, **15**, 1766.

49 E. E. Elemike, I. M. Uzoh, D. C. Onwudiwe and O. O. Babalola, *Appl. Sci.*, 2019, **9**, 499.

50 I. Roy, in *Bioinspired and Green Synthesis of Nanostructures: A Sustainable Approach*, 2023, pp 157–188.

51 N. Manzoor, T. Ahmed, M. Noman, M. Shahid, M. M. Nazir, L. Ali and G. Wang, *Sci. Total Environ.*, 2021, **769**, 145221.

52 H. Ali, M. A. Khan, N. Ullah and R. S. Khan, *J. Photochem. Photobiol., B*, 2018, **183**, 242–250.

53 C. Kaya, M. Ashraf, M. N. Alyemeni and P. Ahmad, *Physiol. Plant.*, 2020, **168**, 345–360.

54 S. K. Kohli, K. Khanna, R. Bhardwaj, E. F. Abd_Allah, P. Ahmad and F. J. Corpas, *Antioxidants*, 2019, **8**, 641.

55 M. A. Khan, B. H. Abbasi, N. Ahmed and H. Ali, *Ind. Crops Prod.*, 2013, **46**, 105–110.

56 B. H. Abbasi, P. K. Saxena, S. J. Murch and C. Z. Liu, *In Vitro Cell. Dev. Biol. Plant*, 2007, **43**, 481–492.

57 G. N. M. Kumar and N. R. Knowles, *Plant Physiol.*, 1993, **102**, 115–124.

58 A. A. Meratan, S. M. Ghaffari and V. Niknam, *Biol. Plant*, 2009, **53**, 5–10.

59 H. A. Zavaleta-Mancera, H. López-Delgado, H. Loza-Tavera, M. Mora-Herrera, C. Trevilla-García, M. Vargas-Suárez and H. Ougham, *J. Plant Physiol.*, 2007, **164**, 1572–1582.

60 S. Sreelatha and P. R. Padma, *Plant Foods Hum. Nutr.*, 2009, **64**, 303–311.

61 Y. Hong, S. Lin, Y. Jiang and M. Ashraf, *Plant Foods Hum. Nutr.*, 2008, **63**, 200–204.

62 A. Salam, J. Qi, X. Fan, A. R. Khan, M. Kah, M. Zeeshan and Y. Gan, *ACS Appl. Mater. Interfaces*, 2025, **17**(25), 36455–36468.

63 M. Kosar, F. Goger and K. H. C. Baser, *Food Chem.*, 2011, **129**, 374–379.

64 B. Aliakbarian, M. Paini, R. Adami, P. Perego and E. Reverchon, *Innovative Food Sci. Emerging Technol.*, 2017, **40**, 2–9.

65 C. Chaves-Lopez, A. Serio, G. Mazzarrino, M. Martuscelli, E. Scarpone and A. Paparella, *Int. J. Food Microbiol.*, 2015, **207**, 49–56.

66 D. M. Kasote, S. S. Katyare, M. V. Hegde and H. Bae, *Int. J. Biol. Sci.*, 2015, **11**(8), 982–991.

67 W. A. Ansari, K. Srivastava, M. Nasibullah and M. F. Khan, *Discover Chem.*, 2025, **2**, 191.

68 J. Delgado-Ospina, M. Martuscelli, C. D. Grande-Tovar, R. Lucas-Gonzáles, J. B. Molina-Hernández, M. Viuda-Martos, J. Fernández-López, J. A. Pérez-Álvarez and C. Chaves-López, *Foods*, 2021, **10**(6), 1243.